



SPECTRAL-DOMAIN OPTICAL COHERENCE TOMOGRAPHY: A NOVEL AND FAST TOOL FOR NDT

M. Wurm¹, K. Wiesauer¹, K. Nagel¹, M. Pircher², E. Götzinger²,
C. K. Hitzenberger² and D. Stifter¹

¹ Upper Austrian Research GmbH, Hafenstrasse 47-51, A-4020 Linz, Austria,
² Centre of Biomedical Engineering and Physics, Medical University of Vienna,
Währingerstr. 13, 1090 Wien, Austria

ABSTRACT

Spectral-domain Optical Coherence Tomography (SD-OCT) is a new, promising variant of OCT, providing superior sensitivity and measurement speed for cross-sectional imaging of turbid materials. OCT, originally developed for applications in the field of biomedical diagnostics, has shown high potential for other non-biomedical investigation tasks, e.g. within the field of non-destructive testing (NDT) and contactless material characterization. However, mostly standard OCT techniques have been used for these applications. Therefore, we demonstrate and evaluate, partly for the first time, the suitability of SD-OCT for selected applications in the field of NDT: contactless imaging of the interior of materials for the determination of the thickness of polymer layers and for the detection of defects in fibre reinforced polymer composites as well as the evaluation of their surface structure is demonstrated. Finally, we investigate the effect of the measurement wavelength on the achievable penetration depth by imaging polymer foam samples with different pore geometries.

KEYWORDS: optical coherence tomography, depth-resolved imaging, non-contact material characterization, polymers, fibre reinforced polymer composites

INTRODUCTION

Optical Coherence Tomography (OCT) is a novel technique for high-resolution non-contact imaging for scattering media. The measurement principle of OCT is based on the interferometric detection of path-length distributions of low-coherence light back-reflected from interfaces within the sample [1]. OCT has been originally developed for imaging of the human retina and its application has been extended to the characterization of a variety of biological tissues, as summarized in recent books and reviews (e.g. [2,3]). Currently, extensive research activities are dedicated worldwide to further develop the OCT method in order to improve imaging quality and to increase the acquisition speed and sensitivity. However, all these techniques and developments are nearly exclusively developed and used for biomedical applications. A summary of the to date reported applications of OCT outside the biomedical field can be found in [4]. It has been shown, that with OCT structures within materials like glass, polymers, ceramics or paper can efficiently be evaluated, showing promising potential for applications in the field of NDT. However, mostly standard OCT setups with rather low resolution and long acquisition times have been used up to now.

Currently, the so called Fourier- (or frequency-) domain OCT (FD-OCT) technique experiences increased attention from the worldwide OCT community [5]. The advantages of this OCT

IVth NDT in PROGRESS

modification are at first that no movable parts are needed for depth scanning, secondly the superior measurement sensitivity and at last the high measurement speed, as laid out in the next section. However, FD-OCT has even less been reported up to now for non-biomedical applications, with one of the few exception related to the determination of varnish thickness on paintings [6]. Therefore, we will present a variety of possible non-biological applications for this new OCT technique in the field of non-destructive testing (NDT) and material characterization.

PRINCIPLE OF OCT AND EXPERIMENTAL SETUP

In Figure 1 a standard OCT setup is depicted. A Michelson interferometer is illuminated with low-coherence light from a broadband lightsource. In the reference arm a movable mirror is placed. By shifting this mirror a depth profile from the sample can be recorded, since interference is only observed, if the optical path of a backscattering structure in the sample arm will coincide with the optical path length in the reference arm. Normally, the envelope of the interference signal is taken to form the depth profile (so-called A scan) at one position on the sample surface. By adjoining several A-scans taken at adjacent locations on the sample (e.g. by scanning the measurement spot with a Galvano-mirror scanner or simply by shifting the sample) cross-sectional images or whole 3D volumes can be acquired. It is worth noting that the lateral resolution, determined by the spot size of the light, is decoupled from the axial (depth) resolution, which is related to the width of the spectrum of the light source: the broader the spectrum, the higher the axial resolution [7].

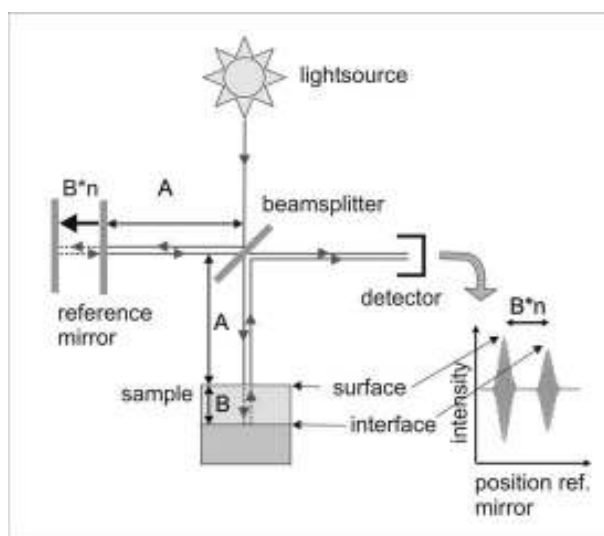


Figure 1: Schema of classical time-domain OCT setup using the Michelson interferometer geometry and a moveable reference mirror. A, B: optical path lengths, n: refractive index of sample layer.

The setup in Figure 1 belongs to the time-domain OCT (TD-OCT) systems: the position of the reference mirror determines the axial measurement location. It is evident that all photons, which are backscattered from other depths than the current axial measurement position, do not contribute to the interference and are lost. In contrast, FD-OCT uses a fixed reference mirror and the spectral distribution of the light exiting the interferometer is analysed. One possibility is depicted in Figure 2, representing a FD-OCT variant called spectral-domain OCT (e.g. [8,9]). The spectrum is taken with a grating spectrometer (with a CCD line camera) and a depth profile is obtained by calculating the

Fourier-transform of the spectrum in the k-space. The acquisition speed of such systems is only limited by the read-out rate of the line sensor, which is routinely in the kHz range, a scan rate which cannot be achieved with the TD-OCT with movable reference mirror. Furthermore, it has been shown that the gain in sensitivity is more than 20 dB for FD-OCT systems when compared to their TD-OCT counterparts [10].

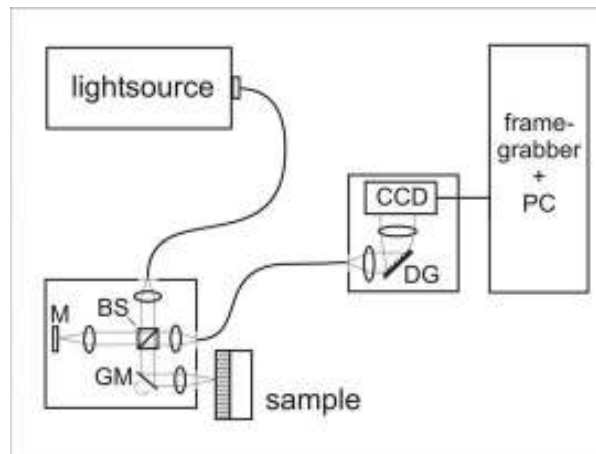


Figure 2: Schematic sketch of a spectral-domain OCT set-up. Abbreviations: beamsplitter (BS), mirror (M), Galvano-scanner mirror (GM), diffractive grating (DG), charge coupled device line camera (CCD).

For our study, we have used two different SD-OCT systems, one operating at a centre wavelength around 800 to 900 nm and one at 1550 nm. The 800 nm system is equipped with a custom-made spectrometer with a fast silicon line-CCD (charge coupled device) camera (2k Pixel, 12 bit), provides a sensitivity of ~ 106 dB with a light power of 1 mW on the sample at an A-scan rate of 28 kHz. As lightsource a single superluminescence diode (SLD) operating at 840 nm, providing a depth resolution of 4 μm in typical materials (refractive index $n \sim 1.5$), or alternatively a multiple SLD-source, providing a depth resolution of 2.7 μm , can be used. The SD-OCT system for 1550 nm operates with a InGaAs line camera (1k Pixel, 12 bit) as line sensor in the spectrometer and a single SLD as lightsource. This SD-OCT system exhibits a sensitivity of more than 102 dB at an A-scan rate of 4 kHz and a depth resolution of 12 μm in typical polymer materials.

RESULTS AND DISCUSSION

In this section we present selected examples to demonstrate the potential of SD-OCT to become a standard non-destructive evaluation tool for various non-biomedical applications. At first, the evaluation of thin film structures is shown in Figure 3. In Figure 3a,b) cross-sectional images from powder coated wood panels, taken at a centre wavelength of 840 nm, are presented. The application of powder coatings on wood is a rather recent one, involving many optimisation steps in the development of the novel powder coatings. The characteristics of the powder coating, like its curing time and temperature, has to be compatible with the used wooden substrates. Furthermore, good adhesion and uniform coating thickness should be achievable. With SD-OCT it is now possible to acquire a cross-sectional image of the coating on the wood within a fraction of a second (in our case 36 ms per image

IVth NDT in PROGRESS

with a size of 1 Megapixel), representing a huge advantage when compared to other (even destructive) methods, like the tedious preparation of micrograph sections to obtain information on the layers. For demonstration purposes, a homogeneously coated wooden surface is compared in Figure 3a) with a sample of minor quality depicted in Figure 3b). For the inhomogeneously coated sample, the layer thickness even decreases in some regions to zero. Furthermore, it is observable, that the powder coating efficiently penetrated the wooden material (white bands below the wood surface in Figure 3b), leaving obviously less material on the surface. An additional example related to the evaluation of thin films can be seen in Figure 3c), showing a polymer foil which has been attached with an adhesive to the underlying support (aluminium coated cardboard). The polymer foil is protecting the interior of a food container and properly follows the support on the left side of the image. In contrast, cellular structures were observed on the right side of the depicted sample area. Here, the layer is partly detached. This region is close to a prefabricated hole which has been cut from the other side in the cardboard to facilitate opening of the container by the consumer.

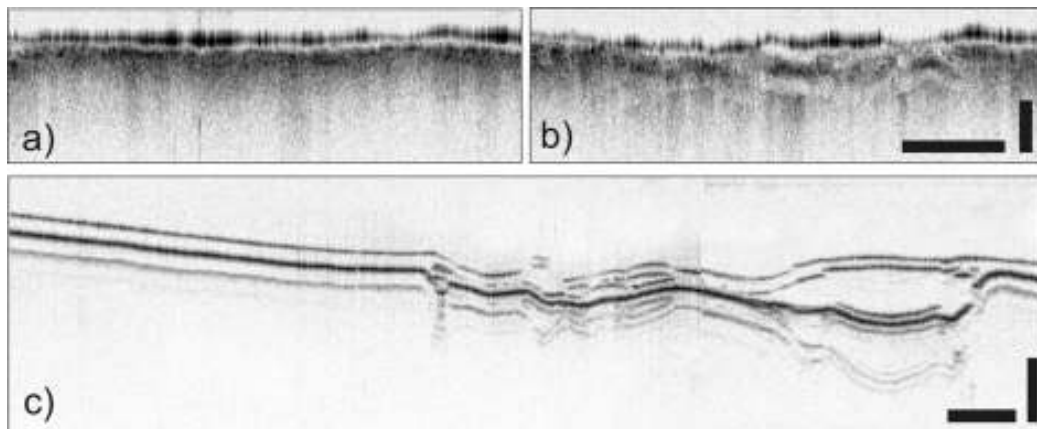


Figure 3: Cross-sectional images taken from layered polymer materials. a),b) powder coating on thermal treated wood, scale bars: 1mm (horizontal), 100 μm (vertical); c) polymer coating on inside of a food container, scale bars: 1 mm (horizontal), 250 μm (vertical).

Introducing a fibre reinforcing structure in a polymer matrix leads to lightweight materials with enhanced material properties for applications e.g. in the aerospace industry. Glass-fibre reinforced polymer (GFRP) composites are routinely used in helicopter rotor blades and the knowledge of damage initiation and propagation is of great interest. It has already been shown that classical TD-OCT is a powerful tool for such characterization tasks [11]. In Figure 4, to the best of our knowledge, the first SD-OCT images for defect detection in GFRP samples are presented. Figure 4a) shows an undamaged region. Clearly, the individual woven fibre tows are visible (e.g. black disks just below the surface represent bundles which are running perpendicular to the image plane). Figure 4b) shows in contrast a damaged region with a delamination situated just below the first fibre layer (marked with arrow) and which occurred after a loading procedure (bending of the sample). It is worth noting, that by exploiting the high acquisition speed of SD-OCT, dynamic studies of crack and damage formation are within reach leading to new insight for a further optimisation of the fibre composites.

In contrast to glass-fibres, carbon fibres are opaque for OCT imaging. Nevertheless, useful information can be obtained on carbon-fibre reinforced polymer (CFRP) composites, as shown in Figure 5.

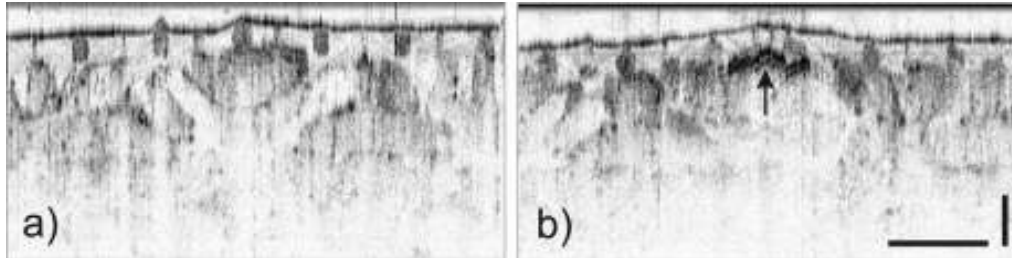


Figure 4: Cross-sectional images taken from a glass-fibre reinforced polymer composite: a) undamaged structure before loading procedure, b) defect region (arrow) after loading. Scale bars: 1 mm (horizontal), 100 μ m (vertical).

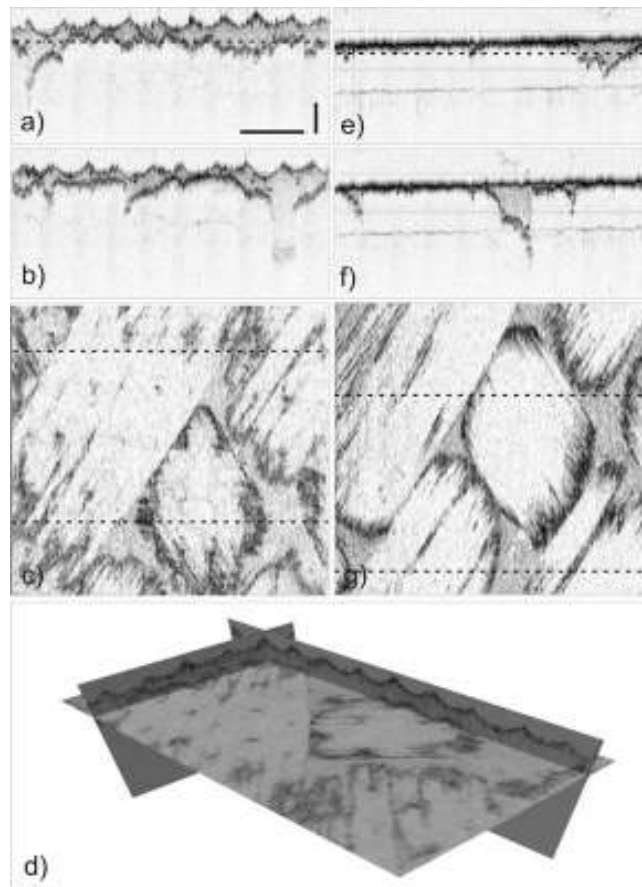


Figure 5: Cross-sectional and en-face images taken from a 3D reconstruction of a surface-near region of CFRP samples. a-d) images taken from a CFRP sample with removed peel-ply, e-f) the same sample after grinding process. The dotted lines in c,g) give the position of the individual cross-sectional and en-face scans of a,b) and e,f), respectively. Scale bars: 1 mm (horizontal), 100 μ m (vertical).

IVth NDT in PROGRESS

Routinely, a so called peel-ply is attached to the surface to facilitate the demoulding process of the CFRP part from the curing form. The peel-ply is then stripped of the surface and leaves a structure as depicted in Figure 5a-d). Clearly, the remaining epoxy material above the first fibre layer is observable. If such a CFRP part is to be bonded, the residual chemical contaminants from the peel-ply fabric, which are still present on the surface, need to be removed. This can be accomplished by simply grinding the surface prior to bonding in order to reach a state as depicted in Figure 5e-g). The superficial epoxy material has been nearly completely removed, with only some remaining epoxy in the areas between the woven bundles. Furthermore, it is evident by comparing the cross-sectional images of Figure 5a,b) with those of Figure 5e,f), that even the topmost regions of the fibre tows have been removed.

All the above images have been acquired with our SD-OCT system operating at 840 nm. In [4] we have shown that the OCT imaging depth can mostly be doubled in turbid polymer by switching to longer wavelength around 1550 nm. The study in [4] has been performed with rather slow TD-OCTs (A-scan rates in the range of one Hertz). In order to improve the imaging speed and to increase the penetration depth, we have built the 1550 nm SD-OCT, as introduced above in the preceding section. In Figure 6, SD-OCT images taken with this system from polymer foam samples with different pore sizes are depicted and compared to their counterparts measured with the 840 nm SD-OCT.

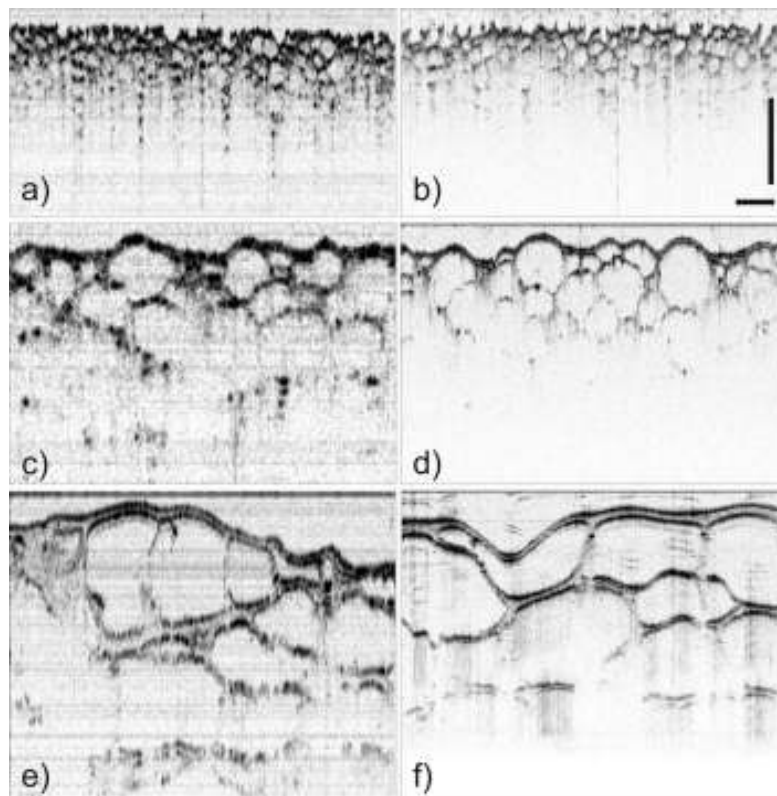


Figure 6: SD-OCT cross-sectional images taken from polymer foam samples with different pore sizes. a),c),e) images taken at a centre wavelength of 1550 nm, b),d),f) taken at 840 nm. Scale bars: 500 μm (horizontal and vertical).

The measurements at 1550 nm in Figure 6 are among the first ever reported SD-OCT images outside biomedical research with an imaging wavelength above 1 μm [12]. It can be seen from them images, that the 840 nm system provides a better depth resolution, due to the characteristics of the used lightsource (broader relative width of the spectrum). On the other hand, the penetration depth of the 1550 nm SD-OCT is slightly better. However, a doubling of the measurement range could not be observed for these cellular materials, as it was the case for the turbid bulk polymer samples investigated in [4]. This might be due to the fact that the impinging light is mostly attenuated by repeated reflections from defined air-polymer surfaces and not by scattering from particles and crystallite boundaries within e.g. turbid polymer matrices.

CONCLUSIONS AND OUTLOOK

We have shown the potential of SD-OCT for applications in the field of NDT and contactless material characterization. Since no movable parts are needed for depth scanning, a compact and robust measurement setup can be built, mandatory for applications in an industrial production environment. A further advantage is the high measurement speed, when compared to former TD-OCT setups. Of special interest is the achievable penetration depth, which can be improved by using longer imaging wavelengths. However, sources with broader spectra will have to be used to preserve axial details as well as novel line array sensors with higher acquisition speed and increased number of pixels, which work in the near infra-red (NIR) region. As an alternative, another FD-OCT variant called swept-source OCT, which uses a narrowband tunable NIR lightsource and only a single photodetector, might be considered for future applications (e.g. [13]). In either way, the recent developments will pave the way for OCT to become a standard measurement tool for applications in the field of NDT.

ACKNOWLEDGEMENTS

We thank Eurocopter Deutschland GmbH (C. Weimer, A. Sauer) for the CFK peel-ply parts and TIGER Coatings GmbH & Co. KG. (T.W. Schmidt, S. Blume) for the powder coated wood samples (from EU FP6 project Holiwood IP011799-2). This work has been financially supported the Austrian Science Fund FWF (Project L126-N08).

REFERENCES

- [1] D. Huang, E. A. Swanson, C.P. Lin, J.S. Schuhman, W.G. Stinson, W. Chang, M.R. Hee, T. Flotte, K. Gregory, C.A. Puliafito, J.G. Fujimoto, "Optical Coherence Tomography", *Science* 254, 1178-1181, 1991.
- [2] Handbook of Optical Coherence Tomography, B.E. Bouma and G.J. Tearney (eds.), Marcel Dekker New York, 2002.
- [3] A.F. Fercher, C.K. Hitzenberger, "Optical coherence tomography", *Progr. Opt.* 44, 215-301, 2002.
- [4] D. Stifter, "Beyond biomedicine: a review of alternative applications and developments for optical coherence tomography", *Appl. Phys. B*, in print.
- [5] A.F. Fercher C.K. Hitzenberger, G. Kamp, S.Y. Elzaiat, „Measurement of Intraocular Distances by Backscattering Spectral Interferometry“, *Opt. Comm.* 117, 43-48, 1995.
- [6] P. Targowski, M. Gora, M. Wojtkowski, *Optical Coherence Tomography for Artwork Diagnostics*, *Laser Chemistry*, Vol. 2006, Article ID: 35373, 2006.
- [7] E.A. Swanson, D. Huang, M.R. Hee, J.G. Fujimoto, C.P. Lin, C.A. Puliafito 1992 High-speed optical coherence domain reflectometry *Opt. Lett.* 17 151-153
- [8] M. Wojtkowski, R. Leitgeb, A. Kowalczyk, T. Bajraszewski, A.F. Fercher, "In-vivo human retinal imaging by Fourier domain optical coherence tomography", *J. Biomed. Opt.* 7, 457-463, 2002.

IVth NDT in PROGRESS

- [9] S. H. Yun, G. J. Tearney, B. E. Bouma, B. H. Park, J. F. de Boer, "High-speed spectral-domain optical coherence tomography at 1.3 μm wavelength", *Opt. Express* 11, 3598-3604, 2003.
- [10] R. A. Leitgeb, C. K. Hitzenberger, A. F. Fercher, "Performance of Fourier domain vs. time domain optical coherence tomography", *Opt. Express* 11, 889-894, 2003.
- [11] J.P. Dunkers, R.S. Parnas, C.G. Zimba, R.C. Peterson, K.M. Flynn, J.G. Fujimoto, B.E. Bouma, "Optical Coherence Tomography of glass reinforced polymer composites", *Composites: Part A* 30 139-145, 1999.
- [12] D. Stifter, K. Wiesauer, M. Wurm, E. Schlotthauer, J. Kastner, M. Pircher, E. Götzinger, C. K. Hitzenberger, "Investigation of polymer and polymer/fibre composite materials with optical coherence tomography", *Meas. Sci. Technol.*, submitted.
- [13] R. Huber, M. Wojtkowski, J. G. Fujimoto, "Fourier Domain Mode Locking (FDML): A new laser operating regime and applications for optical coherence tomography", *Opt. Express* 14, 3225- 3237, 2006.